Nanoparticles

International Edition: DOI: 10.1002/anie.201506469
German Edition: DOI: 10.1002/ange.201506469

Reversible Size Control of Liquid-Metal Nanoparticles under Ultrasonication

Akihisa Yamaguchi, Yu Mashima, and Tomokazu Iyoda*

Abstract: *This paper describes the reversible control of the size of liquid-metal nanoparticles under ultrasonication. Gallium was utilized as a liquid metal, which has a melting point of 29.8 °C. Investigating the effects of ultrasonication (power, time, and temperature) on the formation of gallium nanoparticles revealed that the process is similar to the formation of oil in water (O/W) or water in oil (W/O) emulsions, as the temperature significantly affects the size of the gallium nanoparticles (GaNPs). Under ultrasonication, the balance between the break-up and coalescence of the GaNPs can be adjusted by changing the temperature or adding acid through modulating the natural surface oxide layer (which can be removed with acid) and the stabilizing effect of the surfactant dodecanethiol. Coalescence was predominant at higher temperatures, whereas particle break-up was found to be predominant at lower temperatures. Furthermore, the change in size was accompanied by a shift in the plasmonic absorption of the GaNPs in the UV region.*

Nobel-metal nanoparticles, such as those of gold and silver, have attracted much attention because of their wide variety of applications as plasmonics,[1] catalysts,[2] and sensing materials.[3,4] The control of their size, shape, and structure is essential because of the strong correlation between structural features and properties.[5] The fusion and transformation of preformed smaller nanoparticles into larger nanoparticles or different shapes, including wires, triangles, and sponges, can be induced by a heat treatment,[6] electron beam irradiation,[7] pressurization,[8] or the addition of halides.[9] However, such deformations are usually irreversible. Liquid metals, such as gallium, gallium–indium eutectic alloys (EGaIn: 75 wt% Ga, 25 wt% In), and gallium–indium–tin alloys (Galinstan: 68.5 wt% Ga, 21.5 wt% In, and 10 wt% Sn), which have melting points of 29.8, 15.7 and −19 °C, respectively, have received increasing attention as deformable, moldable, and injectable metals.[10] For example, flexible and stretchable electrodes[11] and antennas[12] based on liquid metals in microfluidic channels have been fabricated, and their functions can be tuned by reversible deformation on the micrometer scale. If such reversible deformations of liquid metals could be realized on the nanometer scale, it may enable new applications with nanostructure-specific functions. However, few studies on the nanostructures of liquid metals have been reported. For example, hemispherical gallium nanoparticle arrays were fabricated by molecular beam epitaxy.[13] The plasmonic substrate was used for UV surface-enhanced Raman scattering (SERS); its UV local enhancement factors were comparable to those achieved with gold or silver nanoparticles ($>10^7$).[13] Ultrasonication is also a facile method to produce liquid-metal nanoparticles from a bulk droplet. Previous reports have shown that alkanethiol-stabilized mercury, EGaIn, and Ga particles with micro- to nanometer sizes can be successfully synthesized through ultrasonication.[14] Furthermore, micro- and nanometer-sized Galinstan liquid-metal marbles stabilized by WO_3 nanoparticles were fabricated by ultrasonication.[15] However, thus far, the reversible deformation of liquid metals on the nanoscale has not been reported. To achieve this objective, we focused on the ultrasonication method that is commonly used for the preparation of oil in water (O/W) or water in oil (W/O) nanoemulsions.[16] In this case, the final droplet size is determined by the two opposite processes of droplet break-up and coalescence.[16] For the liquid-metal nanoparticles, we expected that the size could be reversibly controlled by the balance between these two processes in a similar fashion to the O/W emulsion droplets.

Herein, we report the first example of the reversible size control of liquid-metal nanoparticles under ultrasonication by using gallium as a liquid metal. The break-up and coalescence of the gallium nanoparticles (GaNPs) were controlled with temperature by tuning the amounts of dodecanethiol (C12SH) and by using the surface oxide layer of the GaNPs as a protecting agent that can be removed with hydrochloric acid (HCl). Furthermore, the GaNPs displayed size-dependent plasmonic absorption in the UV region.

The GaNPs were generally prepared as follows: Gallium (100 mg) was added to a 2-propanol solution (5 mL) of C12SH (289 mg), and the solution was sonicated by using a hone-type sonicator (Branson Sonifier 450D; maximum power: 400 W) adjusted to 40% of the maximum power at 20 °C for 120 min, which resulted in a GaNP suspension (see the Supporting Information and Figure S1 for details). A field-emission scanning electron microscopy (FE-SEM) image shows the formation of GaNPs with diameters of approximately 10 to 400 nm (Figure 1 a). The size distribution of the resulting GaNPs has an asymmetric bell shape with a long tail towards larger diameters, characteristic of the log-

[*] Dr. A. Yamaguchi, Prof. Dr. T. Iyoda
Iyoda Supra-integrated Material Project
Exploratory Research for Advanced Technology (ERATO)
Japan Science and Technology Agency (JST)
4259 Nagatsuta-cho, Midori-ku, Yokohama, Kanagawa 226-8503 (Japan)
E-mail: yamaguchi.a.af@m.titech.ac.jp
Y. Mashima
Chemical Resources Laboratory, Tokyo Institute of Technology
4259 Nagatsuta-Cho, Midori-ku, Yokohama, Kanagawa 226-8503 (Japan)

Supporting information for this article is available on the WWW under http://dx.doi.org/10.1002/anie.201506469.

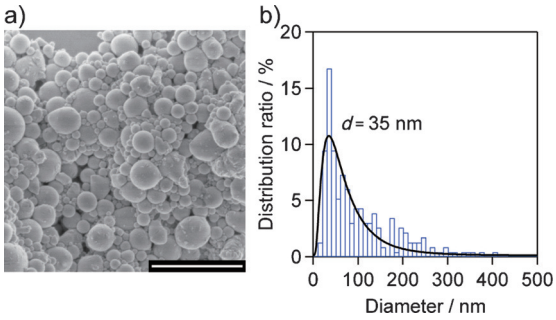

Figure 1. a) FE-SEM image of GaNPs prepared by 40% power ultrasonication at 20°C for 120 min. Scale bar: 1 μm. b) GaNP size distribution. The black solid line is the log-normal fitting curve.

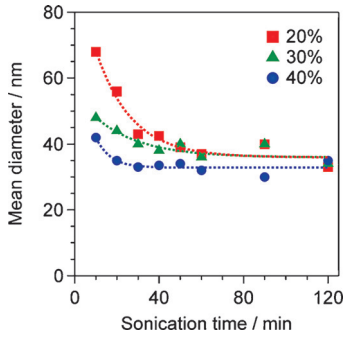

Figure 2. Mean diameters of the GaNPs as a function of ultrasonication time for different ultrasonication powers at 20°C. The dashed lines correspond to monoexponential fitting curves.

normal distributions often observed for emulsion and particle systems (Figure 1b).[17] The value corresponding to the peak of the log-normal fitting curve was used to denote the mean diameter in a similar way to the O/W emulsion droplets. The mean diameter of the GaNPs that were prepared at 40% power ultrasonication for 120 min was thus determined to be 35 nm. Furthermore, 20 and 30% power ultrasonication resulted in mean diameters of 33 and 35 nm, respectively (Figure S2).

Oxygen and carbon were detected to be present on the surface of the GaNPs by energy-dispersive X-ray spectroscopy in combination with transmission electron microscopy (TEM-EDX, Figure S3). Furthermore, X-ray photoelectron spectroscopy gave two peaks at 19.8 and 20.8 eV, which were assigned to gallium suboxide (Ga^{1+}) and gallium oxide (Ga^{3+}), respectively, aside from a peak at 18.7 eV, which corresponds to metallic gallium (Ga^0; Figure S4).[18] These results are due to the fact that the surface of gallium is readily oxidized when the gallium is exposed to ambient atmosphere or even a partial pressure of oxygen as low as 10^{-5} Pa, but the oxidation is spontaneously passivated to form a very thin oxide layer (ca. 2 nm thickness).[10,19] The thin surface oxide layer stabilized the GaNPs even in the absence of C12SH (Figure S5). However, when the oxide-protected GaNPs were again ultrasonicated under acidic conditions (50 mM HCl, approximately 2 equiv with respect to the oxide layer), they immediately coalesced to form a single millimeter-scale sphere (Figure S6) because the thin oxide layer had been easily removed by HCl.[19,20] These observations suggest that both the thin oxide layer and C12SH play important roles as protecting agents during the formation of gallium nanoparticles.

The dependence of the mean diameter of the GaNPs on the ultrasonication time is illustrated in Figure 2. The mean diameters decreased as the irradiation time was increased, and a fraction of larger nanoparticles (ca. 1 μm) was still present after short periods of irradiation, but disappeared after prolonged irradiation (Figure S7). The decrease in size can be fitted to a monoexponential function of the ultrasonication time (see the Supporting Information and Table S1). These results clearly indicate that the minimum diameters reached approximately 35 nm, independent of the ultrasonication power, with prolonged irradiation. However, the time to reach the minimum diameter increased with decreasing ultrasonication power. Delmas and co-workers reported that the minimum size of the O/W emulsion droplets did not depend on the power of ultrasonication, but that the time required to reach this size did. Moreover, the emulsification efficiency depended on the overall energy input into the system.[16c] In a similar fashion, the efficiency of the formation of the gallium nanoparticles depended on the total sonication energy, as shown by plotting the size evolution as a function of the input energy (Figure S8), suggesting some similarities between the nanoparticulate formation of liquid metals and O/W emulsifications. It should be stressed that the GaNPs maintained their liquid state even at 20°C during ultrasonication even though their melting point is 29.8°C. By means of differential scanning calorimetry (DSC), GaNPs prepared at 20°C were shown to have a freezing point of −128.3°C and a melting point of −14.2°C (Figure 3). These results are consistent with previous reports that showed that the confinement of gallium in micro- to nanometer-sized particles resulted in a lowering of the freezing and melting points.[21] Furthermore, the GaNPs maintained this supercooled state for at least two days.

The temperature during ultrasonication is another important factor that influences the emulsification efficiency and the size of the emulsion droplets.[22] Therefore, the effect of

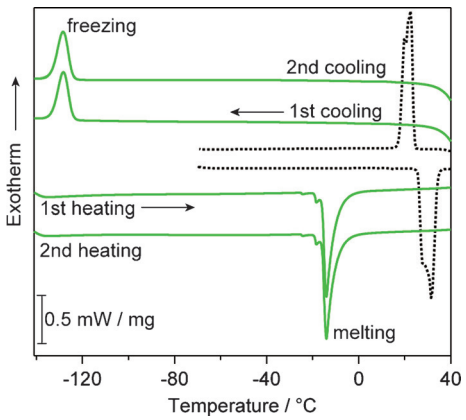

Figure 3. DSC curves of GaNPs (ca. 35 nm) prepared at 20°C by 40% power ultrasonication (green solid line) for the first and second cycles and of bulk gallium (dashed black line) for the first cycle. Scan rate: 10°C min^{-1}.

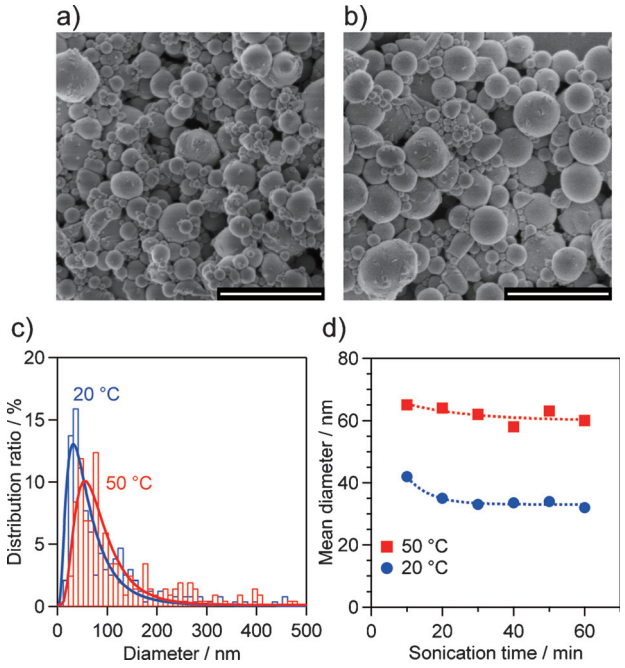

Figure 4. Effect of the sonication temperature on the size of the GaNPs under 40% power ultrasonication. FE-SEM images of GaNPs ultrasonicated at a) 20°C and b) 50°C for 60 min. Scale bars: 1 μm. c) Size distributions of GaNPs prepared by ultrasonication at 20°C (blue) and 50°C (red) for 60 min. Solid lines correspond to the log-normal fitting curves. d) Mean diameters of the GaNPs as a function of sonication time. The dashed lines correspond to monoexponential fitting curves.

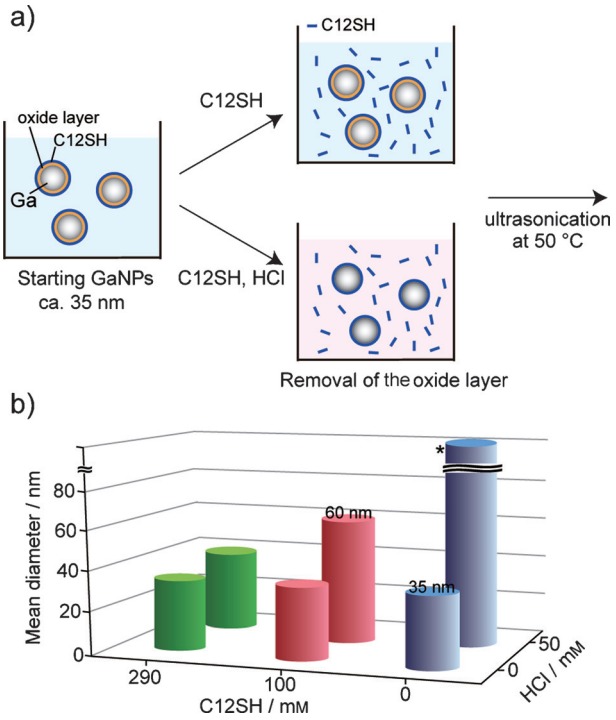

Figure 5. a) Controlling the size of GaNPs. The precursor GaNPs (mean diameter ca. 35 nm) were ultrasonicated in the presence of different concentrations of C12SH (0, 100, or 290 mM) and HCl (0 or 50 mM, approximately 2 equiv with respect to the oxide layer) in 2-propanol (5 mL) at 50°C for 20 min. The precursor GaNPs were prepared by 40% power ultrasonication at 20°C for 20 min. b) Mean diameters of GaNPs processed under the above conditions. * For these conditions, the mean diameter could not be determined because of the wide size distribution, including microparticles.

the sonication temperature on the size of the GaNPs was studied. As observed by FE-SEM (Figure 4a,b), the fraction of larger nanoparticles was larger at 50°C than at 20°C whereas the fraction of smaller nanoparticles was smaller. The mean diameter of the GaNPs formed by ultrasonication at 50°C was approximately 60 nm, which is approximately 1.7 times larger than that at 20°C (Figure 4c). The time to reach the minimum diameter at 50°C is approximately 1.6 times longer than that at 20°C (Figure 4d and Table S1), indicating that the formation of GaNPs is less effective at the higher temperature, possibly because of a decrease of the cavitation effect. In O/W emulsifications, the final droplet size is determined by the balance of two processes, namely droplet break-up and coalescence.[16] The decrease in the viscosity of 2-propanol at higher temperatures will enhance the coalescence rate, which leads to an increase in the size of the GaNPs.[23]

Based on the above evidence, we attempted to control the size of the GaNPs under ultrasonication by varying the sonication temperature. However, once the size had reached its minimum of 35 nm at 20°C, it did not increase even when the temperature was elevated to 50°C. This result is attributed to the strong stabilization of the GaNPs by C12SH and the thin surface oxide layer. Therefore, the size of the GaNPs has to be controlled by tuning their stabilization with C12SH and the oxide layer. For this purpose, an appropriate amount of HCl was added to remove the oxide layer. The concentrations of HCl (0, 50 mM; approximately 2 equiv with respect to the oxide layer) and C12SH (0, 100, or 290 mM) significantly affected the size of the GaNPs (Figure 5). For example, the size of the GaNPs increased from 35 nm to 60 nm in the presence of C12SH (100 mM) and HCl (50 mM). However, ultrasonication in the absence of HCl did not give rise to any changes in the size of the GaNPs regardless of the C12SH concentration. An increased amount of C12SH (290 mM) also disturbed the coalescence even when the oxide layer was removed by addition of HCl (50 mM). In sharp contrast, the nanoparticles no longer maintained their order on the nanometer scale in the absence of C12SH under acidic conditions, resulting in the formation of microscale particles (Figure S9). It is well known that the stability of O/W emulsion droplets significantly depends on the concentration of the surfactant, and reducing the amount of surfactant induces coalescence of the emulsion droplets.[16] Consequently, both C12SH and the oxide layer play important roles as "coalescence regulators" in maintaining the nanometer size of the GaNPs. Furthermore, ultrasonication was also found to be necessary to increase the size of the GaNPs by providing enough power for the coalescence because shaking the sample vial by hand or leaving it to stand induced no change in size.

Finally, the size of the GaNPs was reversibly controlled (Figure 6a). Ultrasonication of the precursor GaNPs (ca.

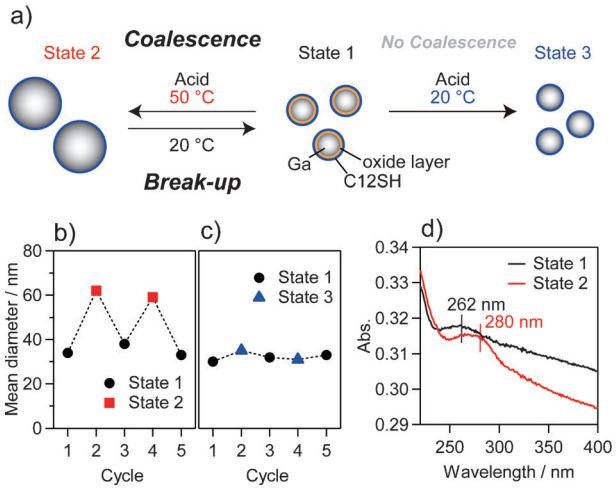

Figure 6. a) Reversibly controlling the size of GaNPs. The precursor GaNPs (mean diameter ca. 35 nm) were ultrasonicated in the presence of HCl (50 mM) and C12SH (100 mM) in 2-propanol (5 mL) at 50 °C (state 1→state 2) or 20 °C (state 1→state 3) for 20 min, and then again at 20 °C for 20 min (state 2 or 3→state 1). The precursor GaNPs were prepared by 40% power ultrasonication at 20 °C for 20 min. b,c) Mean diameters of the GaNPs in states 1–3. d) Absorption spectra of GaNP dispersions corresponding to state 1 (black) and state 2 (red).

35 nm) in the presence of HCl (50 mM) and C12SH (100 mM) at 50 °C resulted in an increase of the mean diameter to approximately 60 nm (state 1→state 2). Next, ultrasonication of the resulting GaNPs at 20 °C led to a decrease in the mean diameter to approximately 35 nm (state 2→state 1). Moreover, this cycle could be repeated (Figure 6b). Meanwhile, the same treatment of the precursor GaNPs at 20 °C induced no significant change in size (state 1→state 3; Figure 6c). Interestingly, the size of the GaNPs significantly affected their plasmonic absorption. As illustrated by the UV absorption spectra of the GaNPs (Figure 6d), a red shift of the plasmonic absorption of the GaNPs from 262 to 280 nm was clearly observed when the size of the GaNPs increased from 35 to 60 nm. The broadness of the plasmonic absorption peaks may be attributed to the polydispersity of the GaNPs.

In conclusion, we have successfully demonstrated for the first time that the size of GaNPs can be reversibly controlled on the nanometer scale upon ultrasonication. Because of some similarities in the formation of gallium nanoparticles and O/W emulsifications, the balance between break-up and coalescence during ultrasonication depends the temperature, and both C12SH and the thin surface oxide layer played essential roles as coalescence regulators. Furthermore, the GaNPs displayed size-dependent plasmonic behavior. We expect that the reversible deformation of plasmonic liquid-metal nanoparticles on the nanoscale rather than on the microscale can enable new applications in plasmonics and other related fields. Further studies along these lines are currently in progress.

Keywords: gallium · liquid metals · nanoparticles · surface plasmon resonance · ultrasonication

How to cite: *Angew. Chem. Int. Ed.* **2015**, *54*, 12809–12813
Angew. Chem. **2015**, *127*, 13000–13004

[1] a) S. Link, M. A. El-Sayed, *J. Phys. B* **1999**, *103*, 4212–4217; b) N. J. Halas, S. Lal, W.-S. Chang, S. Link, P. Nordlander, *Chem. Rev.* **2011**, *111*, 3913–3961.
[2] A. Corma, H. Garcia, *Chem. Soc. Rev.* **2008**, *37*, 2096–2126.
[3] a) S. Nie, S. R. Emory, *Science* **1997**, *275*, 1102–1106; b) C. L. Haynes, A. D. McFarland, R. P. Van Duyne, *Anal. Chem.* **2005**, *77*, 338A–346A.
[4] M. E. Stewart, C. R. Anderton, L. B. Thompson, J. Maria, S. K. Gray, J. A. Rogers, R. G. Nuzzo, *Chem. Rev.* **2008**, *108*, 494–521.
[5] Y. Xia, Y. Xiong, B. Lim, S. E. Skrabalak, *Angew. Chem. Int. Ed.* **2009**, *48*, 60–103; *Angew. Chem.* **2009**, *121*, 62–108.
[6] a) M. M. Maye, W. Zheng, F. L. Leibowitz, N. K. Ly, C.-J. Zhong, *Langmuir* **2000**, *16*, 490–497; b) L. Meli, P. F. Green, *ACS Nano* **2008**, *2*, 1305–1312.
[7] S. Xiong, R. Molecke, M. Bosch, P. R. Schunk, C. J. Brinker, *J. Am. Chem. Soc.* **2011**, *133*, 11410–11413.
[8] H. Wu, F. Bai, Z. Sun, R. E. Haddad, D. M. Boye, Z. Wang, J. Y. Huang, H. Fan, *J. Am. Chem. Soc.* **2010**, *132*, 12826–12828.
[9] a) W. Cheng, S. Dong, E. Wang, *Angew. Chem. Int. Ed.* **2003**, *42*, 449–452; *Angew. Chem.* **2003**, *115*, 465–468; b) A. Rai, A. Singh, A. Ahmad, M. Sastry, *Langmuir* **2006**, *22*, 736–741; c) Z. Zhang, H. Li, F. Zhang, Y. Wu, Z. Guo, L. Zhou, J. Li, *Langmuir* **2014**, *30*, 2648–2659.
[10] M. D. Dickey, *ACS Appl. Mater. Interfaces* **2014**, *6*, 18369–18379.
[11] a) A. C. Siegel, D. A. Bruzewicz, D. B. Weibel, G. M. Whitesides, *Adv. Mater.* **2007**, *19*, 727–733; b) R. K. Kramer, C. Majidi, R. J. Wood, *Adv. Funct. Mater.* **2013**, *23*, 5292–5296.
[12] a) J.-H. So, J. Thelen, A. Qusba, G. J. Hayes, G. Lazzi, M. D. Dickey, *Adv. Funct. Mater.* **2009**, *19*, 3632–3637; b) M. Kubo, X. Li, C. Kim, M. Hashimoto, B. J. Wiley, D. Ham, G. M. Whitesides, *Adv. Mater.* **2010**, *22*, 2749–2752; c) S. Cheng, Z. Wu, *Lab Chip* **2010**, *10*, 3227–3234.
[13] a) P. C. Wu, C. G. Khoury, T.-H. Kim, Y. Yang, M. Losurdo, G. V. Bianco, T. Vo-Dinh, A. S. Brown, H. O. Everitt, *J. Am. Chem. Soc.* **2009**, *131*, 12032–12033; b) Y. Yang, J. M. Callahan, T.-H. Kim, A. S. Brown, H. O. Everitt, *Nano Lett.* **2013**, *13*, 2837–2841.
[14] a) B. Pokroy, B. Aichmayer, A. S. Schenk, B. Haimov, S. H. Kang, P. Fratzl, J. Aizenberg, *J. Am. Chem. Soc.* **2010**, *132*, 14355–14357; b) J. N. Hohman, M. Kim, G. A. Wadsworth, H. R. Bednar, J. Jiang, M. A. LeThai, P. S. Wiess, *Nano Lett.* **2011**, *11*, 5104–5110; c) S. Sudo, S. Nagata, K. Kokado, K. Sada, *Chem. Lett.* **2014**, *43*, 1207–1209.
[15] V. Sivan, S.-Y. Tang, A. P. O'Mullane, P. Petersen, N. Eshtiaghi, K. Kalantar-zadeh, A. Mitchell, *Adv. Funct. Mater.* **2013**, *23*, 144–152.
[16] a) T. Tadros, P. Izquierdo, J. Esquena, C. Solans, *Adv. Colloid Interface Sci.* **2004**, *108–109*, 303–318; b) T. G. Mason, J. N. Wilking, K. Meleson, C. B. Chang, S. M. Graves, *J. Phys. Condens. Matter* **2006**, *18*, R635–R666; c) T. Delmas, H. Piraux, A. C. Couffin, I. Texier, F. Vinet, P. Poulin, M. E. Cates, J. Bibette, *Langmuir* **2011**, *27*, 1683–1692; d) P. Walstra, *Chem. Eng. Sci.* **1993**, *48*, 333–349.
[17] a) C. G. Granqvist, R. A. Buhrman, *J. Appl. Phys.* **1976**, *47*, 2200–2218; b) T. Allen, *Particle Size Measurement*, *3rd ed.* (Ed.: B. Scarlett), Chapman and Hall, London, **1981**.
[18] a) C. D. Wagner, A. V. Naumkin, A. Krout-Vass, J. W. Allison, C. J. Powell, J. R. Rumble, *NIST X-ray Photoelectron Spectroscopy Database*, *3.5th ed.*, **2007**; b) L. Cademartiri, M. M. Thuo, C. A. Nijhuis, W. F. Reus, S. Tricard, J. R. Barber, R. N. S. Sodhi, P. Brodersen, C. Kim, R. C. Chiechi, G. M. Whitesides, *J. Phys. Chem. C* **2012**, *116*, 10848–10860.

[19] M. J. Regan, H. Tostmann, P. S. Pershan, O. M. Magnussen, E. DiMasi, B. M. Ocko, M. Deutsch, *Phys. Rev. B* **1997**, *55*, 10786 – 10790.
[20] a) D. Zrnic, D. S. Swatic, *J. Less-Common Met.* **1969**, *18*, 67 – 68; b) Q. Xu, N. Oudalov, Q. Guo, H. M. Jaeger, E. Brown, *Phys. Fluids* **2012**, *24*, 063101; c) D. Kim, P. Thissen, G. Viner, D.-W. Lee, W. Choi, Y. J. Chabal, J.-B. Lee, *ACS Appl. Mater. Interfaces* **2013**, *5*, 179 – 185.
[21] a) A. Di Cicco, *Phys. Rev. Lett.* **1998**, *81*, 2942 – 2945; b) A. Di Cicco, S. Fusari, S. Stizza, *Philos. Mag. B* **1999**, *79*, 2113 – 2120; c) P. Ghigna, G. Spinolo, G. B. Parravicini, A. Stella, A. Migliori, R. Kofman, *J. Am. Chem. Soc.* **2007**, *129*, 8026 – 8033.
[22] E. Nazarzadeh, S. Sajjadi, *Ind. Eng. Chem. Res.* **2013**, *52*, 9683 – 9689.
[23] G. I. Taylor, *Proc. R. Soc. London Ser. A* **1934**, *146*, 501 – 523.

Received: July 14, 2015
Published online: August 31, 2015

